HOKKAIDO UNIVERSITY

Title	Globular garden beet represents a distinct lineage in the domestication of Beta vulgaris
Author(s)	Hayakawa, Ryo; Taniguchi, Eigo; Oishi, Mion et al.
Citation	BMC Plant Biology, 26 https://doi.org/10.1186/s12870-025-08056-7
Issue Date	2026-01-05
Doc URL	https://hdl.handle.net/2115/98797
Rights(URL)	https://creativecommons.org/licenses/by-nc-nd/4.0/
Type	journal article
File Information	s12870-025-08056-7.pdf

Hokkaido University Collection of Scholarly and Academic Papers : HUSCAP

BMC Plant Biology

RESEARCH Open Access

Globular garden beet represents a distinct lineage in the domestication of *Beta vulgaris*

Ryo Hayakawa[1], Eigo Taniguchi[1], Mion Oishi[1], Sayuri Nishimura[1], Hiroaki Matsuhira[2], Tsubasa Narihiro[2], Yosuke Kuroda[2], Tomohiko Kubo[1] and Kazuyoshi Kitazaki[1*]

Abstract

Background A single plant species can give rise to multiple crop types, but the mechanisms underlying this diversification remain unclear. Clarifying the evolutionary relationships among these crops is a crucial first step in addressing this question. Cultivated beet (*Beta vulgaris* ssp. *vulgaris*) provides a good example, as it includes several distinct crop types, both vegetable and industrial, which are classified into cultivar groups. Among these are the swollen-rooted types, including the garden beet group and the sugar beet group. While the garden beet has traditionally been considered the ancestor of sugar beet, molecular genomic data indicated that the two are actually distantly related within this subspecies. We hypothesized that the genetic diversity of garden beet has been insufficiently characterized to clarify its evolutionary role within cultivated beets. One of our expectations was the discovery of an unrecognized lineage within garden beet genetic resources.

Results We measured 15 taproot traits in 622 plants from 74 garden beet and 7 sugar beet accessions. Hierarchical clustering and principal component analysis of these phenotypic data revealed that the garden beet accessions can be divided into two groups. Visual inspection of the taproot images revealed that the accessions with conical taproots were grouped together with sugar beet, while accessions with globular (as well as other shapes such as cylindrical) taproots formed a separate group. Genomic DNA polymorphism analysis supported this grouping, a noticeable correlation with root morphology. Reanalysis of previous studies revealed that the globular group exhibits reduced mitochondrial polymorphism compared to the conical group. Moreover, garden beet accessions with genomic patterns showing unique demographic separation also displayed globular taproots, pointing to a possible genetic bottleneck during the evolution of this group.

Conclusions These findings indicate that the garden beet group with globular taproots is likely a distinct lineage in the evolution of cultivated beet. We favor the hypothesis that different cultivar groups, such as the (globular) garden beet group and the sugar beet group, originated from a genetically heterogenous population that served as the common ancestor of root-type beet.

Keywords Crop evolution, Domestication, Garden beet, Genetic polymorphism, Population structure, Root morphology, Sugar beet

*Correspondence:
Kazuyoshi Kitazaki
kitazaki@agr.hokudai.ac.jp
[1]Research Faculty of Agriculture, Hokkaido University, Sapporo, Japan
[2]Hokkaido Agricultural Research Center, National Agriculture and Food Research Organization, Memuro, Japan

© The Author(s) 2026. **Open Access** This article is licensed under a Creative Commons Attribution-NonCommercial-NoDerivatives 4.0 International License, which permits any non-commercial use, sharing, distribution and reproduction in any medium or format, as long as you give appropriate credit to the original author(s) and the source, provide a link to the Creative Commons licence, and indicate if you modified the licensed material. You do not have permission under this licence to share adapted material derived from this article or parts of it. The images or other third party material in this article are included in the article's Creative Commons licence, unless indicated otherwise in a credit line to the material. If material is not included in the article's Creative Commons licence and your intended use is not permitted by statutory regulation or exceeds the permitted use, you will need to obtain permission directly from the copyright holder. To view a copy of this licence, visit http://creativecommons.org/licenses/by-nc-nd/4.0/.

Background

Humans have genetically transformed many wild plants into crops, a process known domestication [1]. This process can be highly elaborate, as multiple distinct crops may be developed from a single plant species. Cultivated beet (*Beta vulgaris* ssp. *vulgaris*) is one example, comprising cultivar groups specialized for leaf vegetable, root vegetable, livestock fodder, and sugar production [2]. However, the mechanisms by which these cultivar groups arose (such as the evolutionary relationship) remain unclear. Gaining insight into these processes will help us better understand the genetic potential of plants to adapt to new uses and meet emerging demands [3].

Historical records suggest that the major groups of cultivated beets appeared in the order described below [2]. Leaf beet is believed to be the first domesticated beet, likely selected from sea beet (*B. vulgaris* ssp. *maritima*) during the prehistoric period [2]. Although the root of *B. vulgaris* plants has been used for thousands of years [2], swollen taproots were not documented until the sixteenth century [4]. Iconographic analysis suggests that the earliest swollen-rooted beets had conical taproots [5]. Over time, the morphology of the taproot diversified and gradually evolved towards a more spherical or round shape by the nineteenth century [5]. Fodder beet is thought to be derived from garden beet [4] and exhibits considerable diversity in both color and root morphology [6]. Sugar beet was selected from fodder beets exhibiting white skin, white flesh, and conical root shape [7]. The history of swollen-rooted beet suggests that garden beet is the ancestor of both fodder beet and sugar beet. The emergence of these additional cultivar groups from the sixteenth and seventeenth centuries implies that the garden beet gene pool likely harbored high genetic diversity during this period.

Garden beet (*Beta vulgaris* ssp. *vulgaris* [Garden beet Group]), also known as table beet or beetroot, is cultivated worldwide, but it is especially popular in Europe, North Africa, North- and South America and Oceania [8]. It is consumed both fresh and processed, primarily as a root vegetable, and also harvested for baby leaf production [4]. Garden beet is recognized as a natural source of red dye for food products [8]. Recently, the use of beetroot juice as dietary supplement to enhance athletic performance has contributed to increased garden beet production [9, 10]. Harvest of garden beet is composed of hypocotyl and root tissues, though we refer it as taproot in the present study.

The typical taproot shape of the garden beet is globular, but other forms, such as cylindrical taproot, are also widely cultivated. Other morphologies include long and narrow, as well as flat-shaped taproot [4]. The test Guidelines of the International Union for the Protection of New Varieties of Plants (UPOV) define six types of longitudinal taproot sections and four types of taproot tips as classification criteria (https://www.upov.int/edocs/tgdocs/en/tg060.pdf). While this system provides a fr amework for morphological traits, it is sometimes inappropriate to evaluate genetic resources such as landraces, because they often exhibit atypical morphology. Additionally, environmental factors can affect root morphology. Although previous efforts have attempted to classify garden beet genetic resources [8, 11], the evolutionary relationships among morphological types remain unclear.

Genomic DNA analysis is a key tool for understanding crop evolution [12]. In the case of cultivated beets, several genomes have been sequenced in recent years [13–18]. Based on domestication history, one might expect close genomic relationships among the four major groups. However genomic analyses have yielded unexpected results: while sugar beet and fodder beet genomes group together and the leaf beet genome appears relatively close to them, the garden beet genome forms a more distantly related group [15, 19]. To date, there is no clear explanation for the observed genetic divergence of garden beet from the other cultivated beet groups.

One possible explanation that warrants further investigation is that the genetic diversity within garden beet is broader than previously recognized. This suggests that previous studies may have captured only a limited portion of the garden beet gene pool, rendering them insufficient to fully reconstruct the history of cultivated beets. It is therefore plausible that a missing link remains between garden beet and the other cultivated beet groups. Reconciling the discrepancy between historical records and genomic data represents a critical challenge in the study of crop domestication. A more comprehensive assessment of garden beet genetic resources is therefore essential to improve our understanding of the evolution of swollen-rooted beet. Such insights would also be valuable for ongoing breeding efforts, as new garden beet cultivars continue to be developed and released.

In this study, we investigated garden beet genetic resources at the morphological and genomic DNA levels. Results from these analyses identified two clearly distinct groups in the garden beet gene pool. We discuss the diversification of garden beet cultivars and propose a revised scenario for the evolution of swollen-rooted beet that incorporates these findings.

Results

Measuring taproot to evaluate garden beet genetic resources

Classification of taproot morphology can be subjective when based solely on visual inspection. To address this we implemented an objective, quantitative procedure. We focused on a set of characters listed in Table 1 (see

Table 1 Characters examined in this study

Character		Label of value	Spearman's rank-correlation coefficient (2022 vs. 2023)	*p* (2022 vs. 2023)
Outside of taproot	Number of branched roots	N_{Br}	0.5847	< 0.0001
	Maximum width of hypocotyl or root	*W*	0.3401	0.0103
	Distance from the top of hypocotyl to the *W* layer	*D*	0.3424	0.0098
	Length of hypocotyl	L_{Hyp}	0.47	0.0003
	Length of taproot	L_{Total}	0.655	< 0.0001
	Length of root	$L_{Root} = L_{Total} - L_{Hyp}$	0.6728	< 0.0001
	Area of taproot side view	*A*	0.1198	0.3793
	Ratio of L_{Total} and W_{Max}	L_{Total}/W	0.7093	< 0.0001
	Ratio of *D* and L_{Total}	D/L_{Total}	0.4749	0.0002
	Ratio of L_{Hyp} and L_{Total}	L_{Hyp}/L_{Total}	0.5986	< 0.0001
Inside of taproot	Number of cambia	N_{Cam}	0.5489	< 0.0001
	Area of transverse section at the maximum width of root	S_{Total}	0.4588	0.0004
	Inner area of the third secondary cambium	S_{3cam}	0.4249	0.0011
	Ratio of S_{3cam} and S_{Total}	S_{3cam}/S_{Total}	0.275	0.0403
	Colors of parenchymatous- and vascular zones of roots	*see* Table 3	NA	NA

also Fig. 1), most of which are quantitative, except for the colors of the parenchymatous and vascular zones.

In total, we measured 265 plants from 57 accessions in 2022 and 357 plants from 78 accessions in 2023 (Table 2 and Additional file 1: Table S1).

We examined three to five plants per accession in each year. For each accession, we calculated the yearly average of the measured values (Additional file 2: Table S2). Because expression of quantitative characters is influenced by environmental factors, we assessed whether the measured values could still differentiate among accessions. If these values reflect underlying genetic differences, the ranking of accessions should be consistent between 2022 and 2023. A total of 56 accessions was evaluated in both 2022 and 2023. For each character, we compared the accession ranking between the two years, and calculated Spearman's rank correlation coefficient (Table 1). As a result, 13 out of 14 characters showed statistically significant correlation (p value < 0.05; color traits were excluded from this analysis), indicating that the rankings are consistent between years. These results suggest that the characters listed in Table 1 effectively capture genetic difference among garden beet accessions.

Clusters based on taproot measurements correspond to morphological appearance

We conducted hierarchical clustering to group the accessions based on taproot measurements from the 2023 dataset. The resulting dendrogram revealed two major clusters (Fig. 2). The larger cluster was further subdivided into three subclusters. We designated the two clusters as Clusters I and Cluster II, and subdivided Cluster I into Subclusters Ia, Ib, and Ic.

We also conducted principal component analysis (PCA) using the same data set. The first three principal components explained 40.8%, 21.3%, and 17.8% of the variance, respectively with a cumulative contribution of 79.9% for PC3. The PCA scatter plot shown in Fig. 3 displays two major groups corresponding to Clusters I and II identified in the dendrogram. The three subclusters are also visible but they show some overlap, making their separation less clear in the scatter plot.

We then examined whether any of the specific taproot types were enriched in the clusters or subclusters. The taproots were visually evaluated to identify any morphological trends. Representative images for Subclusters Ia (26 accessions), Ib (19 accessions), Ic (15 accessions) and Cluster II (18 accessions) are shown in Additional Files 7–10: Figure S2-S5. Additionally, Fig. 4 shows images of five representative plants arbitrarily selected from each cluster or subcluster. We observed that many taproots of Cluster II accessions tapered to a point, forming the conical shape characteristic of sugar beet (Fig. 4P-T and Additional Files 10: Figure S5). All sugar beet lines included as controls in this study, except one, were grouped into Cluster II. Subcluster Ia appeared to represent accessions with globular taproots (Fig. 4A-E); however, the globular part primarily consisted of the hypocotyl, with the root portion abruptly thinning just below it. This resulted in a single, very thin root resembling a mouse tail, which was often detached during harvesting. Taproots in Subclusters Ib and Ic were more deformed compared to those in Subcluster Ia. Subcluster Ib included accessions with cylindrical taproots (e.g., Fig. 4F, G and I) and some with

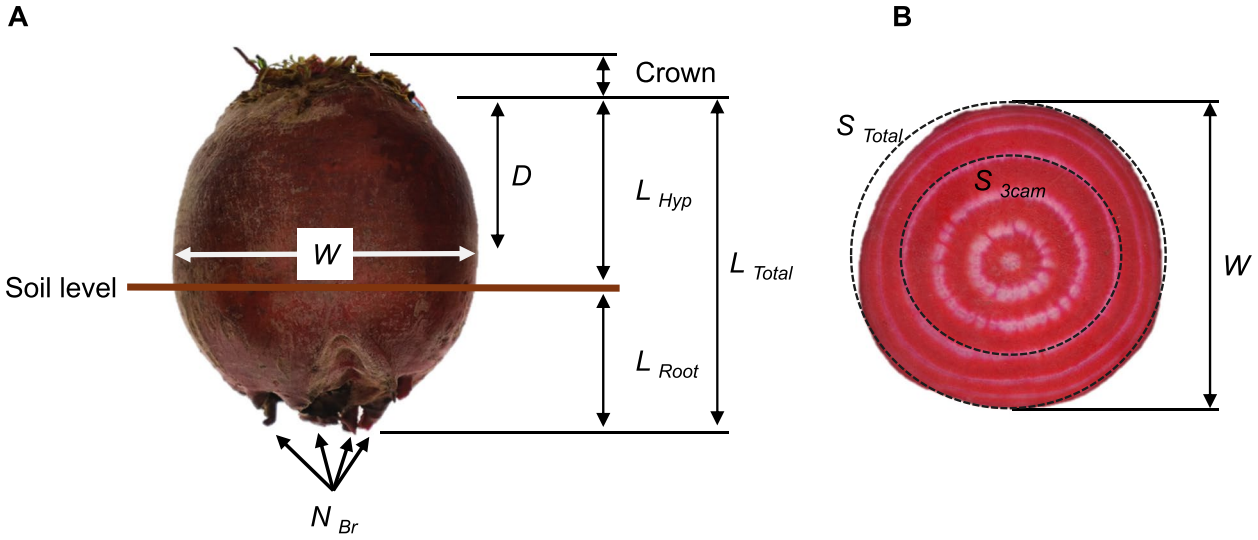

Fig. 1 Measurement of root phenotypes (example shown is BETA 3863). **A**. Side view of the taproot. Soil level is indicated by the brown horizontal line. The extent of the crown, maximum root width (*W*), length of hypocotyl (L_{Hyp}), root length (L_{Root}), and distance from top of hypocotyl to the level of maximum width are indicated (*D*). The number of branched roots (N_{Br}) is marked with arrows. The side area of the taproot does not include the crown. **B**. Transverse section at the point of maximum root width. Number of cambia (N_{Cam}), area of transverse section at the point of maximum root width (S_{Total}), inner area corresponding to the third cambium (S_{3cam}), and pigmentation of parenchymatous and vascular zones of roots were examined from the image

circular truncated shapes (Additional Files 8: Figure S3). Subcluster Ic featured flattened, disc-like taproots (e.g., Fig. 4K and M), in addition to highly deformed ones (e.g., Fig. 4L).

We also performed hierarchical clustering using the 2022 dataset. The resulting dendrogram revealed two major clusters (Fig. 5). The accessions in these two clusters overlap with those of the corresponding 2023 clusters, allowing us to designate them as Clusters I and Cluster II (Table 2) (i.e., Clusters I and II are consistent between 2022 and 2023). This consistency between 2022 and 2023 suggests that the garden beet genetic resources can be divided into two major groups based on taproot measurements values. However, in 2022, Cluster I can be subdivided into two subclusters (shown as IA and IB in Fig. 5), rather than the three observed in the 2023 dendrogram. When comparing 2022 and 2023, we found that the accessions classified as Subcluster Ic in 2023 were predominantly grouped into Subcluster IA in 2022. In contrast, accessions assigned to Subcluster Ia and Ib were distributed across both IA and IB, without a clear pattern. One of the major differences between 2022 and 2023 was the growth period: plants in 2022 were grown for 140 days, compared to 120 days in 2023. It is possible that the extended growth period in 2022 led to overdevelopment in some plants, diminishing the difference in certain traits and affecting subcluster resolution. Hence, we used the 2023 grouping for further analysis.

Root pigmentation

We classified the internal color of taproots in three categories: red or rose (although these two colors were distinguished during data acquisition, they were combined into a single category for this analysis), yellow and white. The presence or absence of pigmentation in the parenchymatous and vascular zones (examples shown in Additional file 11: Figure S6) was assessed separately and recorded. Of the nine possible patterns of pigmentation (i.e., three colors in each of the two zones, $3 \times 3 = 9$), we observed six patterns across 73 garden beet accessions and seven sugar beet lines. The distribution of pigmentation patterns among 616 individual plants —556 garden beets and 60 sugar beets—is shown in Table 3 and Additional file 3: Table S3. The most frequent pattern involved both parenchymatous and vascular zones pigmented in red or rose and was observed in 327 of the 556 garden beet plants (~59%). Overall, red or rose pigmentation in either parenchymatous or vascular zones was highly prevalent, present in 524 of 556 garden beet plants (~94%). Pigmentation heterogeneity was common: 54 of the 73 garden beet accessions (~74%) contained plants exhibiting more than one pigmentation pattern.

We examined whether there is any correlation between pigmentation and root morphology, as defined by cluster or subcluster groupings. Yellow pigmentation was observed in only two accessions, BETA 1448 and BETA 1795, both of which belong to Cluster I (Subcluster Ia). Among the eight garden beet accessions with white (i.e. unpigmented) taproots, all belonged to Cluster I or Cluster II. Of these, two were assigned to Subcluster Ia (BETA 1058 and BETA 1109), one to Subcluster Ib (BETA 179), two to Subcluster Ic (BETA 154 and BETA 3890), and three to Cluster II (BETA 1137, BETA 212 and BETA 334). Overall, we found little evidence of a consistent

Table 2 *Beta vulgaris* accessions used in this study

Accession	Type of beet	Country of origin	Source	Phenotype cluster (2022) (number of plants)	Phenotype cluster (2023) [number of plants]	Population structure	NJ tree clade
Beta vulgaris ssp. *vulgaris*							
BETA 1032	Garden beet	Turkey	IPK [*1]	IA (5)	Ib (5)	Pop3	CLD3
BETA 1034	Garden beet	Turkey	IPK		Ia (5)	Pop4	CLD2
BETA 1037	Garden beet	Georgia	IPK	IB (5)	Ib (5)	Pop1	CLD4
BETA 1058	Garden beet	Germany	IPK	IB (5)	Ia (5)	Pop3	CLD3
BETA 1065	Garden beet	Iran	IPK			Pop3	CLD3
BETA 1104	Garden beet	Greece	IPK		Ic (5)	Pop4	CLD1
BETA 1109	Garden beet	Iran	IPK		Ia (5)	Pop4	CLD5
BETA 1137	Garden beet	Greece	IPK		II (5)	Pop4	CLD1
BETA 1159	Garden beet	Greece	IPK	IA (5)	Ia (5)	Pop4	CLD2
BETA 1165	Garden beet	Greece	IPK	IA (4)	Ic (5)	Pop4	CLD1
BETA 1209	Garden beet	India	IPK		Ib (5)	Pop3	CLD3
BETA 1229	Garden beet	Turkey	IPK	IB (5)	Ib (5)	Pop3	CLD3
BETA 1257	Garden beet	Uzbekistan	IPK	II (4)	Ic (5)	Pop1	CLD4
BETA 1285	Garden beet	Azerbaijan	IPK	IA (5)	Ic (5)	Pop1	CLD4
BETA 1295	Garden beet	Azerbaijan	IPK			Pop1	CLD4
BETA 1306	Garden beet	Greece	IPK	II (4)	II (3)	Pop3	out
BETA 1343	Garden beet	Pakistan	IPK	II (5)	II (5)	Pop2	CLD5
BETA 1388	Garden beet	Soviet	IPK	IA (5)	Ia (5)	Pop1	CLD4
BETA 1448	Garden beet	Iran	IPK		Ia (4)	Pop4	CLD5
BETA 1463	Garden beet	Greece	IPK	IB (5)	Ib (5)	Pop3	CLD3
BETA 1468	Garden beet	Greece	IPK	IB (4)	Ic (5)	Pop3	CLD3
BETA 1478	Garden beet	Greece	IPK	IA (1)	Ic (1)	Pop4	CLD1
BETA 154	Garden beet	Italy	IPK	IA (4)	Ic (5)	Pop4	CLD2
BETA 1541	Garden beet	Turkey	IPK		Ic (5)	Pop4	CLD1
BETA 155	Garden beet	Russia	IPK	IB (5)	Ia (5)	Pop3	CLD1
BETA 1594	Garden beet	Turkey	IPK	IB (5)	Ic (3)	Pop4	CLD2
BETA 1618	Garden beet	Unknown	IPK	IA (5)	II (4)	Pop3	out
BETA 1681	Garden beet	Greece	IPK	IA (5)	Ia (5)	Pop3	CLD3
BETA 1723	Garden beet	Italy	IPK		Ib (5)	Pop3	CLD3
BETA 1744	Garden beet	Greece	IPK	IA (5)	Ia (4)	Pop4	CLD1
BETA 1774	Garden beet	Germany	IPK		Ia (5)	Pop4	CLD1
BETA 1777	Garden beet	Germany	IPK	IB (5)	Ib (5)	Pop3	CLD3
BETA 179	Garden beet	China	IPK	IA (5)	Ib (5)	Pop2	CLD5
BETA 1795	Garden beet	Netherland	IPK	IB (5)	Ia (5)	Pop3	CLD3
BETA 184	Garden beet	Slovakia	IPK	IA (5)	Ic (5)	Pop3	CLD5
BETA 185	Garden beet	Georgia	IPK	IA (5)	Ia (4)	Pop1	CLD4
BETA 186	Garden beet	Georgia	IPK	IB (5)	Ia (5)	Pop1	CLD4
BETA 187	Garden beet	Georgia	IPK	II (5)	II (5)	Pop2	CLD5
BETA 188	Garden beet	Georgia	IPK		Ib (5)	Pop1	CLD4
BETA 189	Garden beet	Georgia	IPK		Ib (4)	Pop1	CLD4
BETA 190	Garden beet	Georgia	IPK		Ia (5)	Pop1	CLD4
BETA 1901	Garden beet	France	IPK		II (5)	Pop2	CLD5
BETA 1911	Garden beet	Greece	IPK		Ia (5)	Pop4	CLD2
BETA 1925	Garden beet	Greece	IPK		Ia (5)	Pop4	CLD1
BETA 2010	Garden beet	India	IPK		Ic (5)	Pop3	CLD3
BETA 2040	Garden beet	Netherland	IPK	IB (4)	Ib (5)	Pop3	CLD3
BETA 2056	Garden beet	France	IPK		II (4)		
BETA 2071	Garden beet	Italy	IPK	IB (5)	Ib (3)	Pop3	CLD3
BETA 212	Garden beet	Georgia	IPK		II (3)	Pop4	CLD5
BETA 2129	Garden beet	USA	IPK	IA (5)	Ia (5)	Pop4	CLD2
BETA 213	Garden beet	Georgia	IPK		Ia (4)	Pop1	CLD4

Table 2 (continued)

Accession	Type of beet	Country of origin	Source	Phenotype cluster (2022) (number of plants)	Phenotype cluster (2023) [number of plants]	Population structure	NJ tree clade
BETA 222	Garden beet	Poland	IPK	IB (4)	Ia (4)	Pop3	CLD3
BETA 223	Garden beet	Georgia	IPK	II (3)	II (4)	Pop2	CLD5
BETA 245	Garden beet	Iraq	IPK	IA (5)	Ib (5)	Pop4	out
BETA 246	Garden beet	Italy	IPK	IB (5)	Ia (5)	Pop4	CLD2
BETA 273	Garden beet	Tajikistan	IPK	IA (5)	Ic (4)	Pop1	CLD4
BETA 33	Garden beet	Canada	IPK	IB (5)	Ib (3)	Pop3	CLD3
BETA 334	Garden beet	Romania	IPK	II (4)	II (4)	Pop2	CLD5
BETA 340	Garden beet	Romania	IPK	IA (5)	Ia (5)	Pop1	CLD4
BETA 341	Garden beet	Romania	IPK		Ia (5)	Pop1	CLD4
BETA 345	Garden beet	Romania	IPK	IA (5)	Ia (5)	Pop1	CLD4
BETA 346	Garden beet	Croatia	IPK	IB (5)	Ib (4)	Pop3	CLD3
BETA 355	Garden beet	Georgia	IPK	IA (4)	Ia (5)	Pop1	CLD4
BETA 357	Garden beet	Italy	IPK	IB (5)	Ia (5)	Pop4	CLD2
BETA 362	Garden beet	Bulgaria	IPK		Ib (5)	Pop3	CLD3
BETA 3818	Garden beet	Cuba	IPK	IA (5)	Ic (4)	Pop3	CLD3
BETA 3861	Garden beet	Georgia	IPK	IA (5)	Ib (4)	Pop1	CLD4
BETA 3863	Garden beet	Georgia	IPK	IB (4)	Ib (5)	Pop1	CLD3
BETA 3879	Garden beet	Georgia	IPK	II (5)	II (5)	Pop1	CLD5
BETA 3881	Garden beet	Georgia	IPK	IA (4)	Ic (5)	Pop1	CLD4
BETA 3890	Garden beet	Poland	IPK		Ic (4)	Pop2	CLD5
BETA 965	Garden beet	Unknown	IPK	IB (5)	Ia (4)	Pop3	CLD1
Crapaudine	Garden beet	France	Natural Harvest [*2]	II (3)	II (5)	Pop2	CLD5
K 7136	Garden beet	Georgia	IPK	II (4)	II (4)	Pop1	CLD5
NK-195 mm-CMS	Sugar beet	Japan	HARC [*3]	II (5)	II (5)	Pop2	CLD5
NK-229 mm-O	Sugar beet	Japan	HARC	II (5)	II (5)		
NK-235 mm-O	Sugar beet	Japan	HARC	II (5)			
NK-291 mm-O	Sugar beet	Japan	HARC	II (4)	II (3)		
NK-294 mm-O	Sugar beet	Japan	HARC	II (5)	II (5)		
NK-307 mm-O	Sugar beet	Japan	HARC	II (5)	II (4)		
NK-328 mm-O	Sugar beet	Japan	HARC			Pop2	CLD5
NK-329 mm-O	Sugar beet	Japan	HARC	II (5)	Ib (5)	Pop2	CLD5
Beta vulgaris ssp. *maritima*							
BETA 248	Sea beet	Spain	IPK	II (4)		Pop2	CLD5
BETA 311	Sea beet	France	IPK			Pop2	CLD5

[*1]The Leibniz Institute of Plant Genetics and Crop Plant Research

[*2]Natural Harvest, Co. Ltd., Japan

[*3]Hokkaido Agricultural Research Center, National Agriculture and Food Research Organization

association between pigmentation pattern and clusters or subclusters classification.

Association between genomic DNA polymorphism and phenotypic clustering

To investigate whether our phenotypic groups based on taproot morphology correspond to underlying genetic structure, we analyzed the genomes of 73 garden beet accessions, three sugar beet lines (NK-195BRmm-CMS, NK-328 mm-O and NK-329 mm-O) and two sea beet accessions (BETA 248 and BETA 311) using ddRAD-seq. A total of 800,943 polymorphic sites were initially identified, including 719,641 single nucleotide polymorphic sites (SNPs) and 81,302 insertions or deletions (indels). After applying quality filters, 7,663 high-confidence SNPs and 775 indels were retained for downstream analysis.

We performed population structure analysis by using the 7,663 SNPs. The optimal number of clusters was determined using ΔK, an ad hoc statistic based on the second-order rate of change in the likelihood function with respect to the number of clusters in the population (K) [20]. The ΔK value reached its maximum value at K = 2, with a secondary peak at K = 4 (Additional file

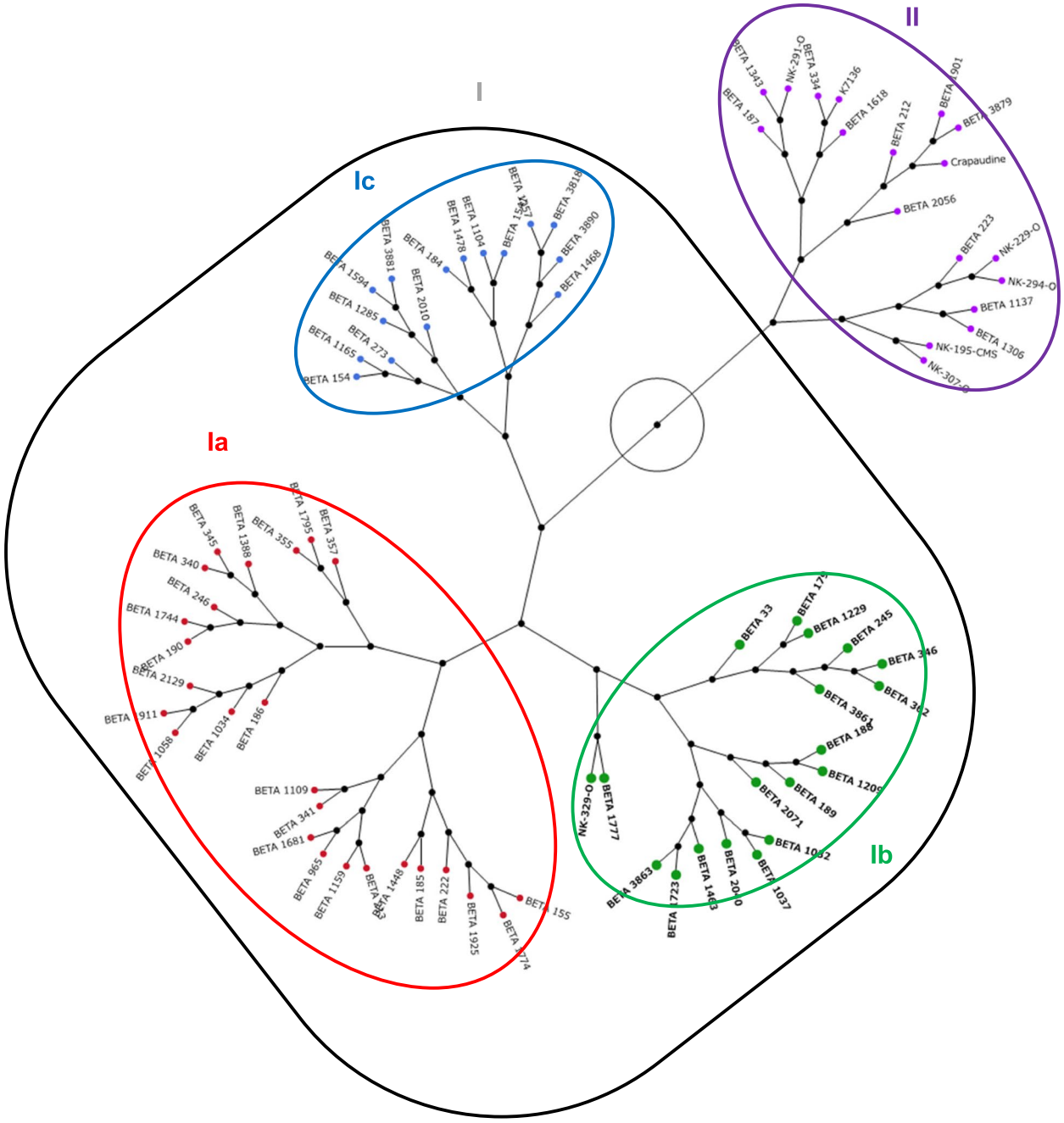

Fig. 2 Dendrogram from hierarchical clustering based on phenotypic values of 14 characters (all characters listed in Table 1 except for root color) measured in 2023. Cluster I is further divided into Clusters Ia, Ib and Ic

12: Figure S7). Bar plots for K = 4 and K = 2 are shown in Fig. 6 and in Additional file 12 (Fig S7), respectively. The four clusters identified at K = 4 were designated Pop1 through Pop4 (Fig. 6). Of the 13 accessions in Pop2, nine are shared with the smaller subpopulation (consisting of 11 accessions) identified at K = 2. Using the same SNP dataset, we also constructed a neighbor-joining tree to examine genetic relationships among accessions (Fig. 7). The tree revealed five distinct clades, named CLD1 through CLD5, along with three solitary accessions that did not group with any of the main clades.

We compared the population structure results (Pop1–Pop4) with the phylogenetic clades (CLD1–CLD5). All Pop2 accessions were grouped within CLD5 (Table 4), which also included a mix of garden beet, sugar beet, and sea beet accessions. Additionally, CLD5 contained several garden beet accessions assigned to Pop1, Pop3 and Pop4. CLD4 was composed exclusively of Pop1 accessions.

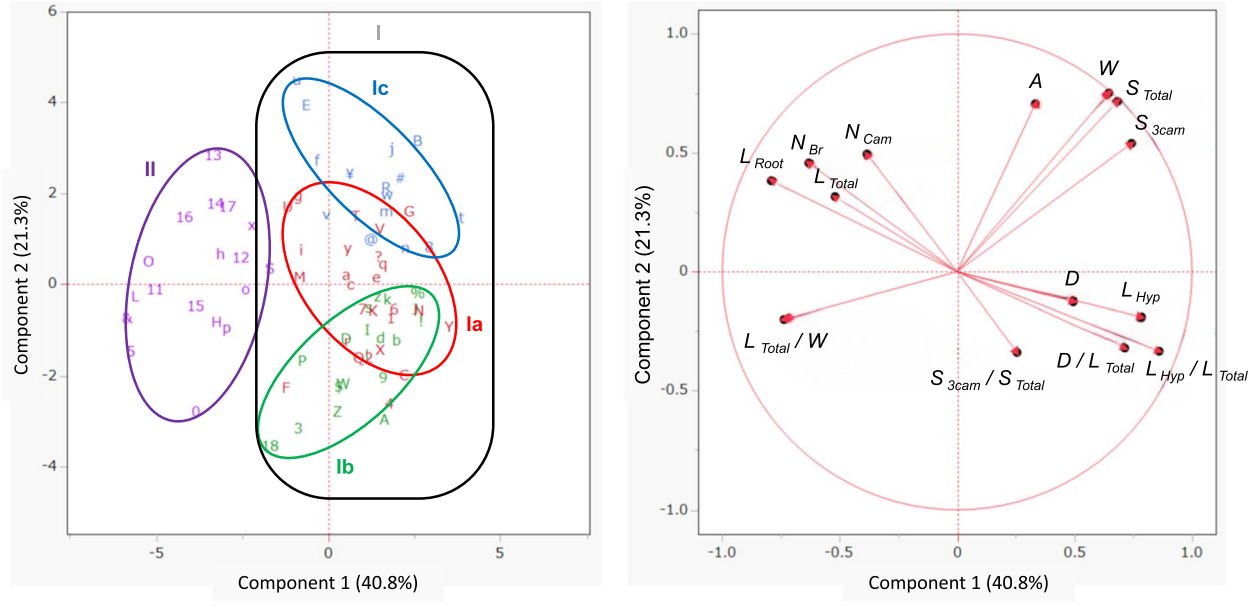

Fig. 3 Principal component analysis of phenotypic data from garden beet genetic resources. Left panel: scatter plot; right panel: biplot. Horizontal and vertical axes represent the first (PC1) and second (PC2) components, respectively. Clusters and subclusters defined in Fig. 2 are circled. Accessions are labeled as follows: A, BETA 33; B, BETA 154; C, BETA 155; D, BETA 179; E, BETA 184; F, BETA 185; G, BETA 186; H, BETA 187; I, BETA 188; J, BETA 189; K, BETA 190; L, BETA 212; M, BETA 213; N, BETA 222; O, BETA 223; P, BETA 245; Q, BETA 246; R, BETA 273; S, BETA 334; T, BETA 340; U, BETA 341; V, BETA 345; W, BETA 346; X, BETA 355; Y, BETA 357; Z, BETA 362; a, BETA 965; b, BETA 1032; c, BETA 1034; d, BETA 1037; e, BETA 1058; f, BETA 1104; g, BETA 1109; h, BETA 1137; i, BETA 1159; j, BETA 1165; k, BETA 1209; l, BETA 1229; m, BETA 1257; n, BETA 1285; o, BETA 1306; p, BETA 1343; q, BETA 1388; r, BETA 1448; s, BETA 1463; t, BETA 1468; u, BETA 1478; v, BETA 1541; w, BETA 1594; x, BETA 1618; y, BETA 1681; z, BETA 1723; 1, BETA 1744; 2, BETA 1774; 3, BETA 1777; 4, BETA 1795; 5, BETA 1901; 6, BETA 1911; 7, BETA 1925; 8, BETA 2010; 9, BETA 2040; 0, BETA 2056;!, BETA 2071;?, BETA 2129; #, BETA 3818; $, BETA 3861; %, BETA 3863; &, BETA 3879; @, BETA 3881; ¥, BETA 3890; 11, Crapaudine; 12, K 7136; 13, NK-195 mm-CMS; 14, NK-229 mm-O; 15, NK-291 mm-O; 16, NK-294 mm-O; 17, NK-307 mm-O; and 18, NK-329 mm-O

The majority of CLD3 accessions corresponded to Pop3, while most accessions in CLD2 and CLD1 belonged to Pop4. Based on these results, we conclude that CLD1 and CLD2 largely correspond to Pop4, CLD3 to Pop3, CLD4 to Pop1, and CLD5 reasonably well to Pop2. Overall, the two analytical methods yielded largely consistent groupings.

To further investigate the relationship between DNA-based and phenotype-based classification groups, we compared the frequencies of the phenotypic groups across the five genomic clades using a contingency table (Fig. 8). Pairwise comparisons revealed that the distribution of phenotypic groups in CLD5 significantly differed from those in CLD4, CLD3 or CLD2. The difference between CLD5 and CLD1 approached significance, with a slightly elevated *p*-value likely attributable to the over-representation of Cluster II accessions in CLD5 (Fig. 8). We also observed significant differences between CLD3 and both CLD1 and CLD2, while the difference between CLD3 and CLD4 was not statistically significant. Notably, the frequency of Subcluster Ib was particularly high in CLD3 compared to the other clades (Fig. 8).

Similarly, the distribution of phenotypic groups in Pop2 significantly differed from that in Pop1, Pop3 or Pop4 (Fig. 8). Pop2 contains the highest number of Cluster II accessions and lacked any Subcluster Ia representatives. In addition, the phenotypic group frequencies differed between Pop3 and Pop4, likely due to the high frequency of Subcluster Ib accessions in Pop3 (Fig. 8).

Taken together, these results suggest an association between Cluster II garden beet accessions and specific DNA-based groups, particularly CLD5.

Discussion

In this study, we evaluated garden beet genetic resources using quantitative measurements of several taproot traits. As a predominantly an outcrossing crop garden beet often exhibits genetic heterogeneity, which contributes to variation in taproot morphology. Furthermore, taproot traits are influenced by environmental conditions and growth period. Despite these sources of variation, our measurements effectively captured accessions-specific characteristics, as indicated by strong correlations in trait ranking across two years. Nevertheless, we recognize that our method could be further optimized to improve both accuracy and efficiency.

The measured values enabled the classification of garden beet genetic resources into two groups. One of these, designated as Cluster II, comprised conical taproots, a trait shared by our sugar beet lines. This raises the

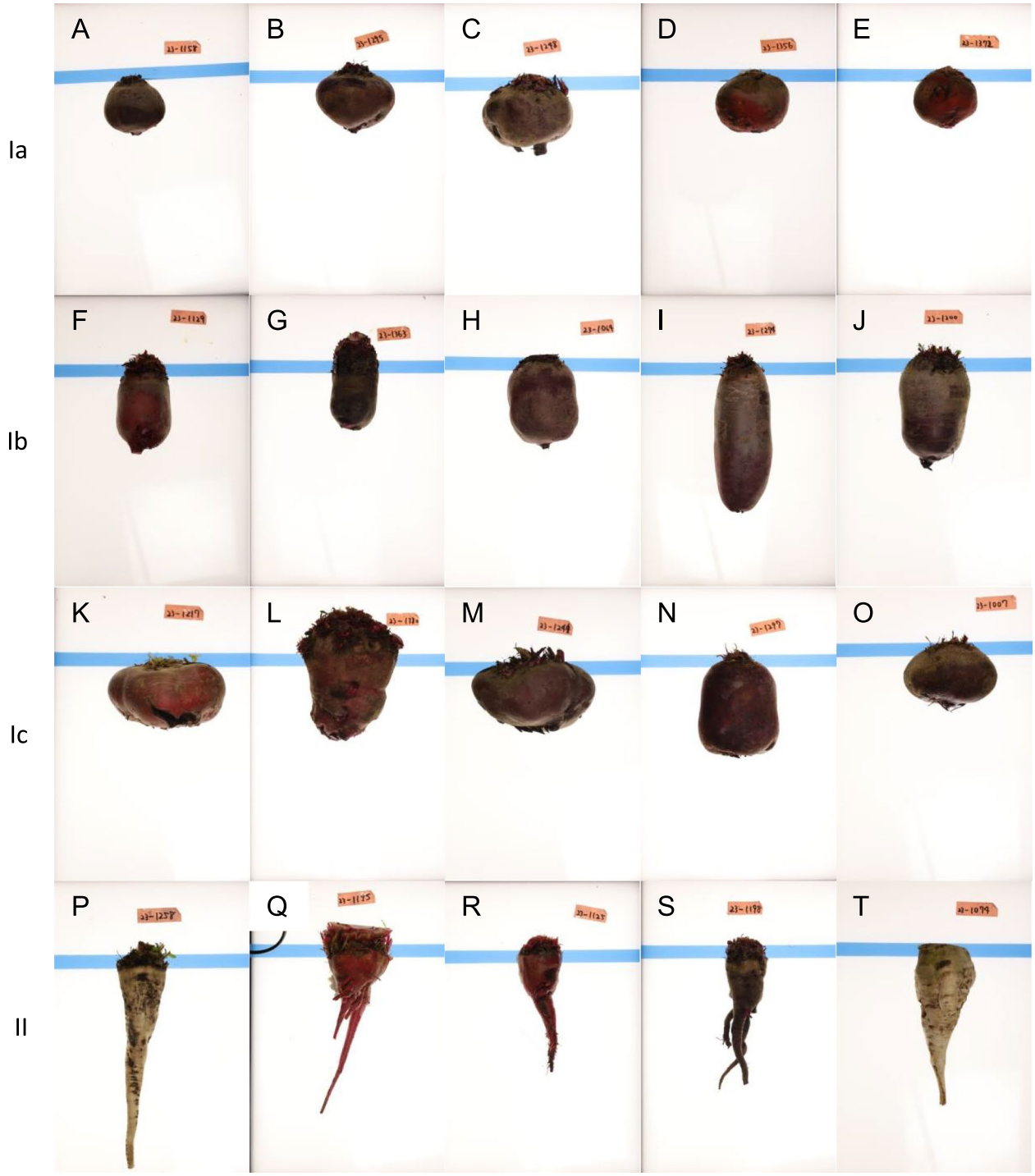

Fig. 4 Taproots of five representative plants from each Clusters/Subclusters. Names of Clusters/Subclusters are shown on the left. The width of the blue tape in photographs is 19 mm. Accessions are labeled as follows: A, BETA 155; B, BETA 186; C, BETA 190; D, BETA 246; E, BETA 1448; F, BETA 179; G, BETA 245; H, BETA 362; I, BETA 1777; J, BETA 2040; K, BETA 154; L, BETA 184; M, BETA 1165; N, BETA 1468; O, BETA 2010; P, BETA 212; Q, BETA 1618; R, BETA 3879; S, Crapaudine; and T, NK-195 mm-CMS

possibility that some accessions within our garden beet collection may have been misidentified or mislabeled. However, the presence of a commercial variety, 'Crapaudine', within cluster II supports the validity of this group as a genuine subset of garden beet. Notably, 'Crapaudine' is a heirloom cultivar with a long history [21].

According to the PCA biplot (Fig. 3B), we infer that root length (L_{Root}), along with composite traits that

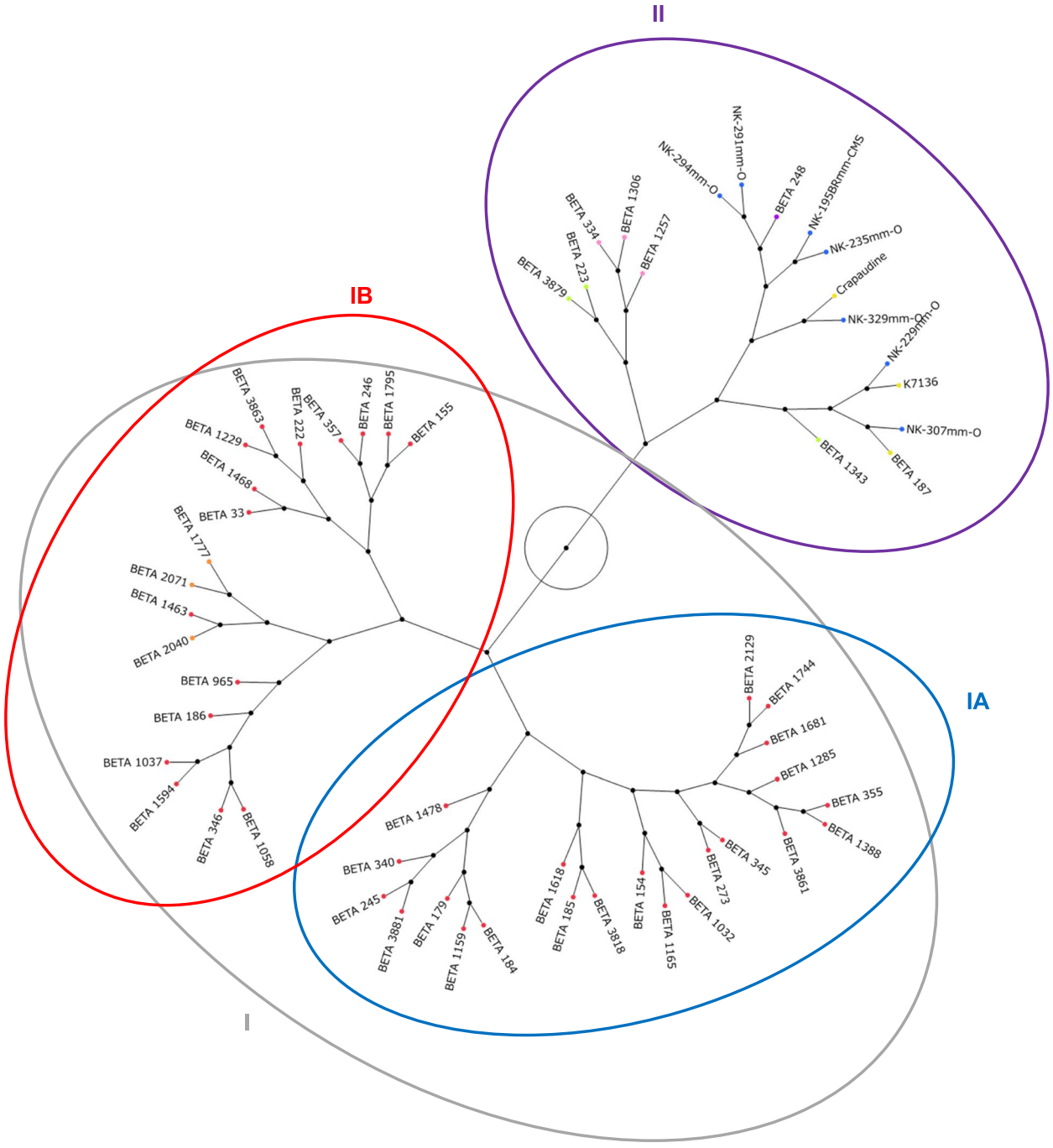

Fig. 5 Dendrogram of hierarchical clustering based on phenotypic values of 14 characters (those listed in Table 1 except for root color) in 2022. Two large clusters, I and II, are shown along with subclusters IA and IB within cluster I

include L_{Root} as a component, significantly contributed to the formation of Cluster II. In contrast, accessions having a large hypocotyl contribute to Cluster I (Fig. 3B). During harvesting, fine roots of Cluster I accessions were often lost whereas the thicker roots of Cluster II accessions remained intact. This observation suggests that the primary difference between Cluster I and Cluster II may be related to root thickening. It is also possible that the genetic mechanisms underlying hypocotyl swelling and root swelling are distinct.

Accessions in Subcluster Ic tend to exhibit high values for side area of the taproot (A) and for traits related to cross-sectional area—specifically width (W), total area (S_{Total}), and area inside of the third secondary cambium (S_{3cam}). This likely explains the enrichment of accessions with wide, flattened taproots in this subcluster. In

Table 3 Distribution of root pigmentation patterns

		Vascular Tissue			Total
		Red or rose	White	Yellow	
Parenchymatous Tissue	Red or rose	327	196	0	523
	White	1	81	0	82
	Yellow	0	7	4	11
Total		328	284	4	616

contrast, cylindrical taproots are characteristic of Subcluster Ib; however, it remains unclear why the ratio of S_{Total} and S_{3cam} contributes to the definition of this subcluster. Further detailed analyses of taproot development are needed to clarify these patterns. It is also noteworthy that each cluster and subcluster includes atypical accessions that differ markedly from other group members. Thus, the morphological characterization of garden beet taproots remains a complex and ongoing challenge, including the choice of parameters that can be used to characterize taproot morphology.

The garden beet genetic resources examined in this study were pigmented in red or rose. Segregation of pigmentation patterns was observed in ~ 74% of the accessions, suggesting that the genes controlling pigmentation have not been fixed yet in many of them. Yellow pigmentation was very rare and found exclusively in accessions belonging to Subcluster Ia. However, additional examples are necessary to confirm that yellow pigmentation is truly confined to Subcluster Ia. Several genes controlling pigmentation have been identified in garden beet [22, 23]; these could help addressing the question why red pigmentation is predominant in this species.

Our study revealed a close association between morphological groupings and genome DNA-based groupings. We found that most of the Cluster II accessions, characterized by a conical taproot morphology, were confined to CLD5, indicating that garden beet accessions with this taproot morphology form a group genetically distinct from those with other forms. A similar conclusion was drawn by Dhiman et al. [24]. In general, the morphological clusters encompassed multiple DNA-based groups (Fig. 8). However, accessions in Cluster I tended to show wide distribution across the genome-based groups. This pattern was more pronounced in the population structure analysis than in the NJ tree. One possible explanation is an environmental effect, such as soil condition, on root morphology, potentially leading to altered or insufficient expression of the accession's genetic potential. Alternatively, similar taproot morphologies may have evolved independently, or genes affecting root morphology may have introgressed into some lineages.

Kanomata et al. [25] analyzed mitochondrial polymorphism in some of the accessions used in this study. We reanalyzed their data to examine the relationship between mitochondrial polymorphism and phenotypic clusters and calculated diversity indices (Additional file 4: Table S4). The results showed diversity indices values of 0.1442 for Cluster I and 0.7586 for Cluster II, indicating that accessions with a conical taproot (Cluster II) are more polymorphic in terms of mitochondrial variations than those with other taproot shapes (Cluster I). Kanomata et al. [25] proposed that minor mitochondrial types—contributing to the observed polymorphism—may be a remnant of introgression from other beet types such as leaf beet and sea beet. We consider this a plausible explanation, particularly because crossing root-type beet with leaf beet has been shown to produce offspring with various taproot shapes, including conical ones [26]. An alternative possibility is that garden beet genetic resources with conical taproots represent a prototype of cultivated garden beet. The earliest illustration of swollen-rooted beet depicts a conical shape [5], closely resembling Cluster II accessions. Globular beets, which would likely fall into Cluster I, appeared later [5]. The reduced mitochondrial polymorphism in Cluster I accessions could reflect a genetic bottleneck associated with this morphological transition. This notion is supported by the observation that allelic polymorphism of the nuclear gene *restorer of fertility 1* is markedly reduced in

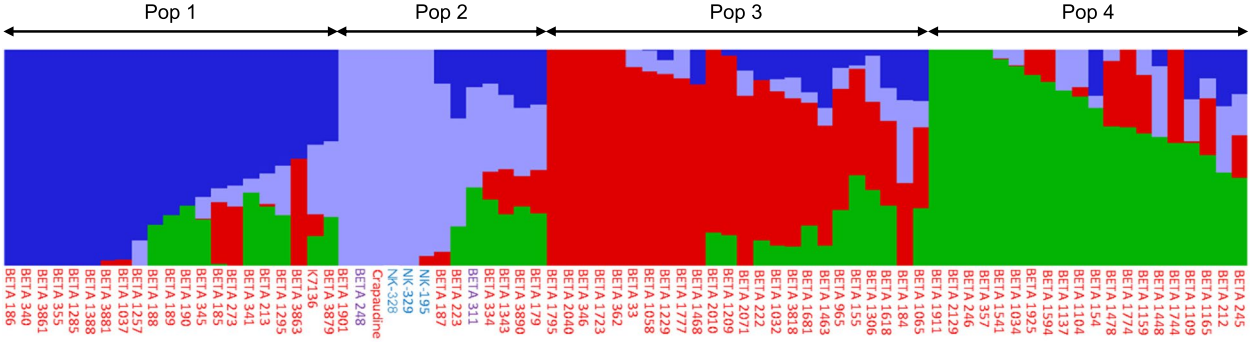

Fig. 6 Bar plot showing the results of population structure analysis based on SNPs identified by ddRAD-seq. Four genetic populations (Pop1 to Pop4) are indicated. Garden beet, sugar beet and sea beet accessions are labeled in red, blue and purple letters, respectively

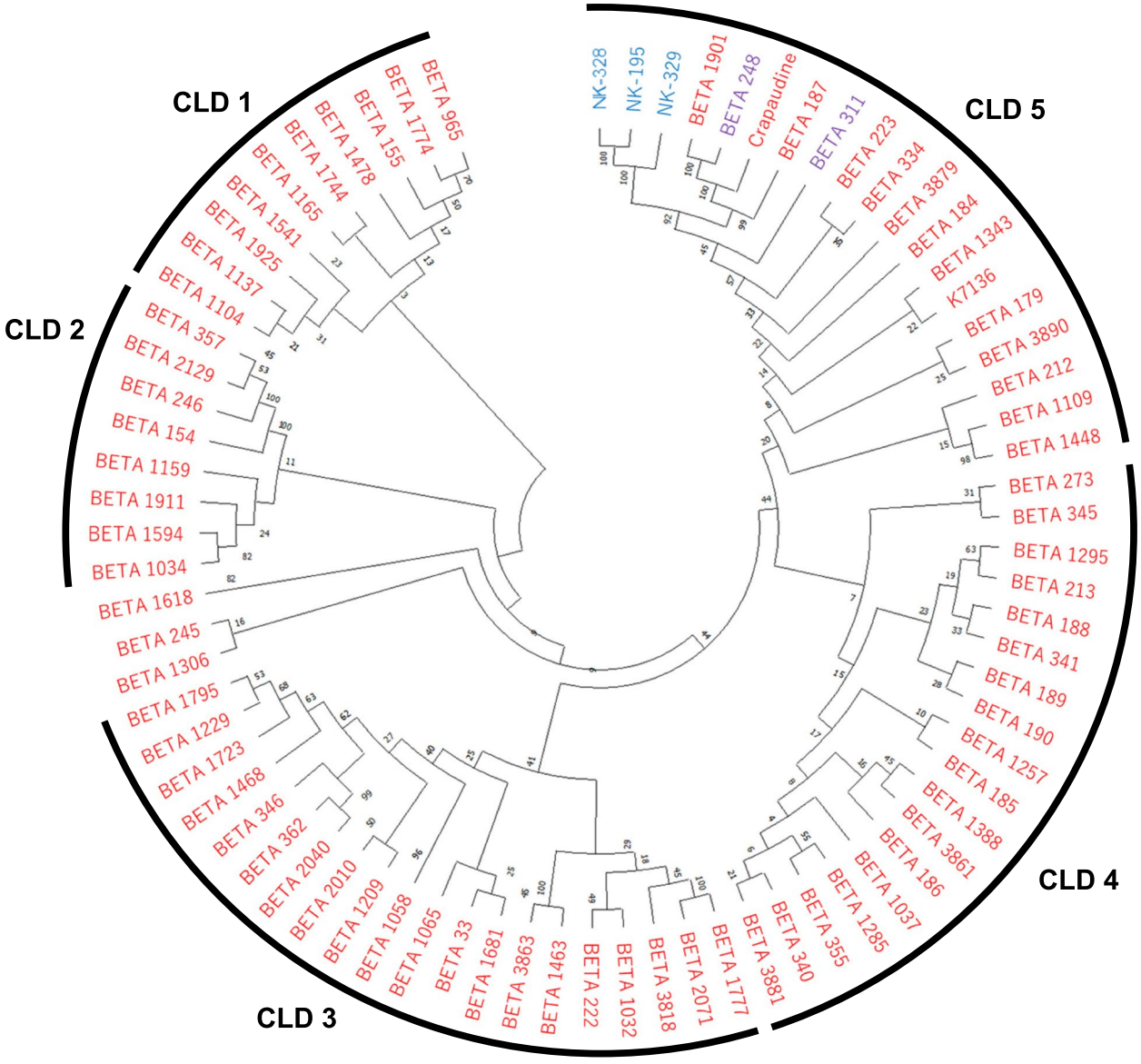

Fig. 7 Neighbor-joining tree using SNPs identified by ddRAD-seq. Five clades are designated CLD1 through CLD5. Accessions BETA 1618, BETA 245 and BETA 1306 do not group within any clade. Garden beet, sugar beet and sea beet accessions are indicated by red, blue and purple letters, respectively

Table 4 Phylogenetic clades and corresponding populations of garden beet accessions

		Populations				
		Pop1	**Pop2**	**Pop3**	**Pop4**	**Total**
Phylogenetic clade	CLD1			2	8	10
	CLD2				8	8
	CLD3	1		19		20
	CLD4	18				18
	CLD5	2	13	1	3	19
	Solitary acc			2	1	3
	Total	21	13	24	20	78

A

	Ia	Ib	Ic	II	Total
CLD 1	5	0	4	1	10
CLD 2	6	0	2	0	8
CLD 3	4	12	3	0	19
CLD 4	9	4	4	0	17
CLD 5	2	2	2	10	16
sol	0	1	0	2	3
Total	26	19	15	13	73

B

	Ia	Ib	Ic	II	Total
Pop1	9	5	4	2	20
Pop2	0	2	1	7	10
Pop3	6	11	4	2	23
Pop4	11	1	6	2	20
Total	26	19	15	13	73

Fig. 8 Contingency tables showing the relationship between phenotypic clusters and clades in the neighbor-joining tree (**A**) or populations in the barplot (**B**). The number of garden beet accessions is indicated. Statistically significant pairs after Holm correction ($\alpha < 0.05$) are indicated by brackets with asterisks

garden beet compared to sugar beet [27], suggesting that Cluster I may represent a more derived lineage. It should be noted that further genomic analyses, involving careful selection of beet accessions, will be necessary to confirm genetic bottlenecking.

Interestingly, previous genome-wide analyses of garden beet varieties (e.g. [15, 19, 28],) also indicate a genetic bottleneck. For example, Galewski and McGrath [15] noted that garden beet cultivars such as 'Bulls Blood' and 'Detroit Dark Red'—both of which have globular taproots and fall within Cluster I—were genetically distinct from leaf beet, fodder beet and sugar beet varieties. By estimating historical effective population size, they showed that these garden beet cultivars experienced a different demographic history, possibly shaped by strong selection, compared to other beet types [15].

The Cluster II accessions were part of CLD5, the same group to which our sugar beet accessions belong. This indicates that some garden beet accessions are genetically similar to sugar beet. If Cluster II represents the prototype garden beet, it is plausible that root-type beet has diverged into two lineages with this prototype as a common origin: one lineage leading to globular garden beet types through selection from conical forms, and another leading to sugar beet. However, the domestication of cultivated beet is known to be a very complex process involving extensive introgression among different beet types [4]. The sugar beet lines used in this study represent only part of the morphological diversity and other forms, such as more cylinder-shaped, are known. Therefore, genomic analyses of cylinder-like sugar beet accessions will be necessary to clarify the relationship between sugar beet and garden beet. To fully elucidate the evolutionary history and diversification of garden beet and other root-type beets, comprehensive analyses of genes, genomes and genetic resources are required.

Conclusion

The taproots of the garden beet genetic resources examined in this study showed substantial morphological variations, including conical, globular, cylindrical, and flat forms. Our data suggest that these accessions can be classified into at least two groups. One of the two groups was enriched in conical shaped taproots, whereas the other primarily comprised accessions with globular or other non-conical shapes. Notably classification based on genomic DNA showed partial concordance with these morphological groupings. Furthermore, garden beet accessions with conical taproots clustered together with some conical sugar beet lines at both the morphological and genomic levels.

By integrating previously published mitochondrial polymorphism data [25] with our clustering results, we found that the conical taproot group is markedly more polymorphic than the globular group (the latter showing less than one fifth of the mitochondrial diversity). A prior genomic study that detected a unique bottleneck-like effect in the garden beet genomes had analyzed only globular shaped garden beet cultivars. Iconographic evidence suggests that conical garden beet types appeared as early as the sixteenth century, whereas spherical or round garden beets do not appear before the nineteenth century.

Taken together, these observations support the hypothesis that globular garden beet represents a selected subset from a genetically heterogenous group represented by conical garden beet, from which sugar beet evolved as a distinct lineage. This notion implies that the domestication of cultivated beet did not follow a single trajectory (leaf -> garden -> sugar) but instead diverged at some point during evolution. Our data therefore point to the existence of a genetically heterogenous root-type beet group from which multiple cultivar lineages emerged.

Methods

Plant materials

B. vulgaris accessions used in this study are listed in Table 2. *B. vulgaris* ssp. *vulgaris* (Garden beet Group) accessions were obtained from The Leibniz Institute of Plant Genetics and Crop Plant Research (IPK) or purchased online. All *B. vulgaris* ssp. *vulgaris* (Sugar beet Group) lines were developed by Hokkaido Agricultural Research Center, National Agriculture and Food Research Organization, Japan. Two wild beet (sea beet,

B. vulgaris ssp. *maritima*) accessions are included in this study. Seedlings were first grown in a greenhouse and then transplanted to the Experimental Farm, Field Science Center for Northern Biosphere, Hokkaido University.

Taproot phenotyping

Harvested plants were washed in water before removing leaves and fine roots. Images of the harvested taproots were captured by using digital cameras, EOS RP RF24-105 IS STM and PowerShot G9 X Mark II (Canon, Tokyo, Japan). Four side-view images were taken from each harvested taproot. We examined a total of 15 morphological traits as summarized in Table 1 (see also Fig. 1). The crown was defined as the part extending from the top of the harvest to the last leaf scar (Fig. 1). The hypocotyl was defined as the part extending from the bottom end of the crown to the point where the first fine root appeared, indicated as the 'soil level' in Fig. 1. The remaining part of the harvested organ was defined as the root. Visible taproot characteristics were examined as follows: the number of roots was counted using the side view-images and hypocotyl length was measured from the images using ImageJ (https://imagej.net/ij/) [29]. Images were also processed using Python 3.8 scripts (Additional Files 6: Figure S1) to examine the additional characters outside the taproot. The background and crown were masked in black to isolate the taproot (Additional Files 13: Protocol S1). The image of taproot was converted into white and the contour was smoothened (Additional Files 13: Protocol S1). From the obtained image, the following morphological values were extracted in pixels: length of taproot, distance from the top of hypocotyl to the layer of the maximum width, and area of taproot side view. These pixel values were converted into centimeters using a size marker.

Taproots were then transverse sectioned at their point of maximum width using a knife, and the sections were scanned with a flatbed scanner (400-SCN025, Sanwa Supply, Okayama, Japan). Internal taproot traits were assessed as follows: the number of cambial rings —*B. vulgaris* forms multiple secondary cambia [28]—was counted from scanned images; the color of the root parenchymatous and vascular zones was visually classified as red, rose, white, or yellow. Combinations of colors and pigment distribution were assigned a code from 1 to 16; for example, accessions in which both parenchymatous and vascular tissues were red were given code 1 (see Tables S1 and S2). The total area of the transverse section and the inner area enclosed by the third secondary cambium [30] were calculated from scanned images using ImageJ.

Statistical analysis

Statistical analyses were conducted using JMP Pro ver.17.0.0 (JMP Statistical Discovery LLC, Cary, NC, USA). Measured values were Box-Cox transformed and normalized. Principal component analysis (PCA) was done using list-wise deletion. Hierarchical clustering was done using Ward's method. Fisher's exact test was performed online (http://aoki2.si.gunma-u.ac.jp/exact/fisher/getpar.html), *p*-values were adjusted using the Holm method in Microsoft Excel (Microsoft Japan, Tokyo, Japan).

Double digest restriction-site associated DNA sequencing (ddRAD-seq)

Green leaves from three to five plants per accession were pooled and ground in liquid nitrogen using a mortar and pestle. Genomic DNA was isolated using the NucleoSpin Plant II (Takara Bio, Kusatsu, Japan). DNA samples were digested with two restriction enzymes MspI and EcoRI, and adapters were ligated to the resulting fragments following the protocol of Bioengineering Lab. Co., Ltd. (Sagamihara, Japan). Paired-end sequencing (100- or 150 bp) was performed on a DNBSEQ-G400 (MGI Tech Japan, Tokyo, Japan). A summary of the data is presented in Additional file 5: Table S5. Reads quality was assessed using FastQC (https://www.bioinformatics.babraham.ac.uk/projects/fastqc). Bases Phred scores below 30 were trimmed using Sickle (https://github.com/najoshi/sickle). Adapter sequences were removed with Trimmomatic-0.39 (http://www.usadellab.org/cms/) [31] using the following parameters: ILLUMINACLIP:DNBSEQ-PE.fa:2:30:10, LEADING:30, TRAILING:30, SLIDINGWINDOW:4:15, and MINLEN:30.

Identification of variant nucleotides and genotyping

Processed reads were mapped onto the sugar beet reference genome of EL10-1.0 [14] using the BWA software (https://github.com/lh3/bwa) [32]. Variant sites were called in VCF format files using GATK HaplotypeCaller (https://gatk.broadinstitute.org/hc/en-us) [33]. Sites with a depth (DP) ≥ 6 and Genotype Quality (GQ) ≥ 10 were retained using VCFtools (http://vcftools.github.io/index.html) [34]. Joint genotyping was performed using GATK GenomicsDBImport and GenotypeGVCFs. Polymorphic sites were identified through the following steps: (1) retaining sites with call rate > 0.6 using VCFtools; (2) imputing genotype with Beagle 5.4 (https://faculty.washington.edu/browning/beagle/beagle.html) [35]; (3) extracting biallelic sites using PLINK 1.9 (www.cog-genomics.org/plink/1.9/) [36]; (4) filtering sites with a minor allele frequency (MAF) > 0.03 using VCFtools; (5) retaining sites with Hardy–Weinberg equilibrium *p*-value > 0.0001 using PLINK 1.9; and (6) excluding sites

in linkage disequilibrium with adjacent loci ($R^2 > 0.5$) using PLINK 1.9.

Genetic analysis

Population structure was analyzed using ADMIXTURE 1.3 (https://dalexander.github.io/admixture/index.html) [37] with a bootstrap value of 1000. The resulting bar plot was visualized using R 4.3.2 (https://www.R-project.org/). Of the 7,663 identified SNPs, 4,920 homozygous sites were selected to generate representative nucleotide sequences for each accession. A FASTA file for phylogenetic analysis was created using VCF-kit (https://vcf-kit.readthedocs.io/en/latest/). Sequence alignment was performed using MUSCLE, and phylogenetic analysis was conducted with MEGA X (https://www.megasoftware.net/) [38] using default settings. Mitotype data were obtained from Kanomata et al. (2022) [25], and mitotype polymorphism was summarized by calculating the diversity index *H* [39] in Microsoft Excel.

Supplementary Information

The online version contains supplementary material available at https://doi.org/10.1186/s12870-025-08056-7.

Additional file 1: Table S1. Phenotypic values of beet plants examined in this study.

Additional file 2: Table S2. Phenotypic values of beet genetic resources examined in this study (mean ± SD).

Additional file 3: Table S3. Pigmentation patterns and number of plants.

Additional file 4: Table S4. Mitotypes reported in Kanomata et al. (2022).

Additional file 5: Table S5. Summary of ddRAD sequencing.

Additional file 6: Figure S1. An example of image processing in this study. A. Original side-view image taken with a digital camera. The boundary between the crown and hypocotyl is marked by a blue line. B. The background and crown were darkened to highlight the taproot, using the script ExtractROI_2023.py. C. The image was rotated to make the crown–hypocotyl boundary horizontal, using the script turn_90_and_trimming_2023.py. D. The taproot image was converted to white and its contour was smoothened, using the script getmidline_and_maxwidth_2023.py.

Additional file 7: Figure S2. Morphology of hypocotyls and roots of garden beet genetic resources belonging to cluster Ia. A, BETA 155; B, BETA 185; C, BETA 186; D, BETA 190; E, BETA 213; F, BETA 222; G, BETA 246; H, BETA 340; I, BETA 341; J, BETA 345; K, BETA 355; L, BETA 357; M, BETA 965; N, BETA 1034; O, BETA 1058; P, BETA 1109; Q, BETA 1159; R, BETA 1388; S, BETA 1448; T, BETA 1681; U, BETA 1744; V, BETA 1774; W, BETA 1795; X, BETA 1911; Y, BETA 1925; and Z, BETA 2129.

Additional file 8: Figure S3. Morphology of hypocotyls and roots of garden beet genetic resources and a sugar beet line belonging to cluster Ib. A, BETA 33; B, BETA 179; C, BETA 188; D, BETA 189; E, BETA 245; F, BETA 346; G, BETA 362; H, BETA 1032; I, BETA 1037; J, BETA 1209; K, BETA 1229; L, BETA 1463; M, BETA 1723; N, BETA 1777; O, BETA 2040; P, BETA 2071; Q, BETA 3861; R, BETA 3863; and S, NK-329mm-O.

Additional file 9: Figure S4. Morphology of hypocotyls and roots of garden beet genetic resourcesbelonging to cluster Ic. A, BETA 154; B, BETA 184; C, BETA 273; D, BETA 1104; E, BETA 1165; F, BETA 1257; G, BETA 1285; H, BETA 1468; I, BETA 1478; J, BETA 1541; K, BETA 1594; L, BETA 2010; M, BETA 3818; N, BETA 3881; and O, BETA 3890.

Additional file 10: Figure S5. Morphology of hypocotyls and roots of garden beet genetic resources and sugar beet lines belonging to cluster II. A, BETA 187; B, BETA 212; C, BETA 223; D, BETA 334; E, BETA 1137; F, BETA 1306; G, BETA 1343; H, BETA 1618; I, BETA 1901; J, BETA 2056; K, BETA 3879; L, Crapaudine; M, K 7136; N, NK-195mm-CMS; O, NK-229mm-O; P, NK-291mm-O; Q, NK-294mm-O; and R, NK-307mm-O.

Additional file 11: Figure S6. Phenotypic patterns of root pigmentation. Accession names, images of root sections, and colors of parenchymatous- and vascular zones are shown.

Additional file 12: Figure S7. Results of population structure analysis of garden beet genetic resources used in this study. ΔK statistic for each K value (number of populations). The vertical and horizontal axes represent ΔK and K, respectively. B. Bar plot showing population structure at K = 2.

Additional file 13: Protocol S1. Procedures for image processing by Python 3.8 scripts.

Acknowledgements

Part of this study was conducted at the Field Science Center for the Northern Biosphere, Hokkaido University.

Authors' contributions

Conceptualization: Ryo Hayakawa, Tomohiko Kubo and Kazuyoshi Kitazaki Data curation: Ryo Hayakawa, Eigo Taniguchi, Mion Oishi, and Sayuri Nishimura Formal analysis: Ryo Hayakawa and Eigo Taniguchi Funding acquisition: Yosuke Kuroda, Tomohiko Kubo, and Kazuyoshi Kitazaki Methodology: Ryo Hayakawa, Eigo Taniguchi, and Kazuyoshi Kitazaki Project administration: Tomohiko Kubo and Kazuyoshi Kitazaki Resources: Hiroaki Matsuhira, Tsubasa Narihiro, Yosuke Kuroda Supervision: Tomohiko Kubo Validation: Ryo Hayakawa, Eigo Taniguchi, and Tomohiko Kubo Visualization: Ryo Hayakawa, Eigo Taniguchi, and Tomohiko Kubo Writing – original draft: Ryo Hayakawa, Eigo Taniguchi, and Tomohiko Kubo Writing – review & editing: Tomohiko Kubo and Kazuyoshi Kitazaki.

Funding

This work was supported by the Japan Society for the Promotion of Science, Grant-in-Aid for Scientific Research (JP21H02159 and JP24K01726 to H. Matsuhira, K. Kitazaki and T. Kubo, JP22K05569 to H. Matsuhira and K. Kitazaki, and JP25K22354 to Y. Kuroda, K. Kitazaki and T. Kubo).

Data availability

All raw sequencing data are available in the DDBJ Sequence Read Archive under BioProject accession PRJDB37582, as runs DRR752419–DRR752496 (DRA accession DRA022634).

Declarations

Ethics and Consent to Participate declarations

Not applicable.

Competing interests

The authors declare no competing interests.

Received: 8 October 2025 / Accepted: 24 December 2025
Published online: 05 January 2026

References

1. Prugganan MD. What is domestication? Trends Ecol Evol. 2022;8:663–71.
2. Biancardi E: Cultivated offspring. In: Biancardi E, Panella LW, McGrath JM, editors. *Beta maritima*. The Origin of Beets. 2nd ed. Cham: Springer Nature Switzerland AG; 2020:219–236.
3. Zhang J, Yu H, Li J. *De novo* domestication: retrace the history of agriculture to design future crops. Curr Opin Biotechnol. 2023;81:102946.
4. Goldman IL, Navazio JP. History and breeding of table beet in the United States. In: Janick J, editor. Plant Breeding Reviews, vol. 22. Hoboken: John Wiley & Sons; 2003. p. 357–88.
5. Goldman IL, Janick J. Evolution of root morphology in table beet: historical and iconographic. Front Plant Sci. 2021;12:689926.

6. Biancardi E, Lewellen RT: History and current importance. In: Biancardi E, Panella LW, McGrath JM, editors. Beta maritima. The Origin of Beets. 2nd ed. Cham: Springer Nature Switzerland AG; 2020:1–48.
7. Winner C. History of the crop. In: Cooke DA, Scott RK, editors. The Sugar Beet Crop. London: Chapman & Hall; 1993. p. 1–35.
8. Goldman IL, Navazio JP: Table beet. In: Prohens J, Nuez F, editors. *Vegetables I. Asteraceae, Brassicaceae, Chenopodiaceae, and Cucurbitaceae. Handbook of Plant Breeding*. Heidelberg: Springer; 2008:219–238.
9. Traverse JH. Beet It. Circ Res. 2018;123:635–7.
10. Abu-Ellail FFB, Salem KFM, Saleh MM, Alnaddaf LM, Al-Khayri JM: Molecular breeding strategies of beetroot (*Beta vulgaris* ssp. *vulgaris* var. *conditiva* Alefeld). In: Al-Khayri JM, Jain SM, Johnson DV, editors. *Advances in Plant Breeding Strategies: Vegetable Crops. Volume 8: Bulbs, Roots and Tubers*. Cham: Springer Nature Switzerland AG; 2021:157–212.
11. Baranski R, Grzebelus D, Frese L. Estimation of genetic diversity in a collection of the garden beet group. Euphytica. 2001;122:19–29.
12. Alam O, Purugganan MD. Domestication and the evolution of crops: variable syndromes, complex genetic architectures, and ecological entranglements. Plant Cell. 2024;36:1227–41.
13. Dohm JC, Minoche AE, Holtgräwe D, Capella-Gultiérrez S, Zakrzewski F, et al. The genome of the recently domesticated crop plant sugar beet (*Beta vulgaris*). Nature. 2014;505:546–9.
14. Funk A, Galewski P, McGrath JM. Nucleotide-binding resistance gene signatures in sugar beet, insights from a new reference genome. Plant J. 2018;95:659–71.
15. Galewski P, McGrath JM. Genetic diversity among cultivated beets (*Beta vulgaris*) assessed via population-based whole genome sequences. BMC Genomics. 2020;21:189.
16. Lehner R, Blazek L, Minoche AE, Dohm JC, Himmelbauer H. Assembly and characterization of the genome of chard (*Beta vulgaris* ssp. *vulgaris* var. *cicla*). J Biotechnol. 2021;333:67–76.
17. Wascher FL, Stralis-Pavese N, McGrath JM, Schulz B, Himmelbauer H, Dohm JC. Genomic distances reveal relationships of wild and cultivated beets. Nat Commun. 2022;13:2021.
18. Felkel S, Dohm JC, Himmelbauer H. Genomic variation in the genus *Beta* based on 656 sequenced beet genomes. Sci Rep. 2023;13:8654.
19. Andrello M, Henry K, Deveaux P, Verdelet D, Desprez B, Manel S. Insights into the genetic relationships among plants of *Beta* section *Beta* using SNP markers. Theor Appl Genet. 2017;130:1857–66.
20. Evanno G, Regnaut S, Goudet J. Detecting the number of clusters of individuals using the software STRUCTURE: a simulation study. Mol Ecol. 2005;14(8):2611–20.
21. Bonavent J-F, Bessone L, Geny A, Berville A, Denizot J-P, et al. A possible origin for the sugar beet cytoplasmic male sterility source Owen. Genome. 1989;32:322–7.
22. Hatlestad GJ, Sunnadeniya RM, Akhavan NA, Gonzalez A, Goldman IL, et al. The beet R locus encodes a new cytochrome P450 required for red betalain production. Nat Genet. 2012;44:816–20.
23. Hatlestad GJ, Akhavan NA, Sunnadeniya RM, Elam L, Cargile S, et al. The beet Y locus encodes an anthocyanin MYB-like protein that activates the betalain red pigment pathway. Nat Genet. 2015;47:92–6.
24. Dhiman AS, Taliadoros D, Stukenbrock EH, McGrath JM, Emrani N, et al.: Signatures in domesticated beet genomes pointing at genes under selection in a sucrose-storing root crop. bioRxiv 2024. https://doi.org/10.1101/2024.05.27.596033.
25. Kanomata Y, Hayakawa R, Kashikura J, Satoh K, Matsuhira H, et al.: Nuclear and mitochondrial DNA polymorphisms suggest introgression contributed to garden beet (*Beta vulgaris* L.) domestication. Genet Resour Crop 2022, Evol 69:271–283.
26. Fischer HE. Origin of the 'Weisse Schlesische Rübe' (white Silesian beet) and resynthesis of sugar beet. Euphytica. 1989;41:75–80.
27. Taniguchi E, Kanomata Y, Tanaka H, Oishi M, Hayakawa R, et al. Differences in *restorer-of-fertility 1* haplotype polymorphism are associated with crop history of garden beet and sugar beet (*Beta vulgaris* L.). Genet Resour Crop Evol. 2025;72:6689–701.
28. Mangin B, Sandron F, Henry K, Devaux B, Willems G, Devaux P, et al. Breeding patterns and cultivated beets origins by genetic diversity and linkage disequilibrium analyses. Theor Appl Genet. 2015;128:2255–71.
29. Schneider CA, Rasband WS, Eliceiri KW. NIH image to ImageJ: 25 years of image analysis. Nat Methods. 2012;9:671–5.
30. Elliott MC, Weston GD. Biology and physiology of the sugar-beet plant. In: Cooke DA, Scott RK, editors. The Sugar Beet Crop. London: Chapman & Hall; 1993. p. 37–66.
31. Bolger AM, Lohse M, Usadel B. Trimmomatic: a flexible trimmer for Illumina sequence data. Bioinformatics. 2014;30(15):2114–20.
32. Li H, Durbin R. Fast and accurate short read alignment with Burrows-Wheeler transform. Bioinformatics. 2009;25:1754–60.
33. McKenna A, Hanna M, Banks E, Sivachenko A, Cibulskis K, Kernytsky A, et al. The genome analysis toolkit: a MapReduce framework for analyzing next-generation DNA sequencing data. Genome Res. 2010;20:1297–303.
34. Danecek P, Auton A, Abecasis G, Albers CA, Banks E, Mark A. DePristo MA, et al.: The variant call format and VCFtools. Bioinformatics 2011, 27:2156–2158.
35. Browning BL, Zhou Y, Browning SR. A one-penny imputed genome from next generation reference panels. Am J Hum Genet. 2018;103:338–48.
36. Chang CC, Chow CC, Tellier LC, Vattikuti S, Purcell SM, Lee JJ. Second-generation PLINK: rising to the challenge of larger and richer datasets. Gigascience. 2015;4(1):s13742–015-0047-8.
37. Alexander DH, Novembre J, Lange K. Fast model-based estimation of ancestry in unrelated individuals. Genome Res. 2009;19:655–1664.
38. Kumar S, Stecher G, Li M, Knyaz C, Tamura K. MEGA X: molecular evolutionary genetics analysis across computing platforms. Mol Biol Evol. 2018;35:1547–9.
39. Ishii T, Takahashi C, Ikeda N, Kamijima O, Mori N. Mitochondrial microsatellite variability in common wheat and its ancestral species. Genes Genet Syst. 2006;81:211–4.

Publisher's Note

Springer Nature remains neutral with regard to jurisdictional claims in published maps and institutional affiliations.